# Switching Error Modes of QCA Circuits

Sanjukta Bhanja* and Sudeep Sarkar†
* Electrical Engineering †Computer Science and Engineering
University of South Florida, Tampa, Florida.
Emails: bhanja@eng.usf.edu, sarkar@cse.usf.edu

***Abstract*— The Quantum-dot Cellular Automata (QCA) model offers a novel nano-domain computing architecture by mapping the intended logic onto the lowest energy configuration of a collection of QCA cells, with two possible ground states for each cell. A four phased clocking is used to keep the computations at the ground state throughout the circuit. Computing errors in QCA circuits can arise due to the failure of the clocking scheme to switch portions of the circuit to its new ground state with change in input. To study these switching errors we need to consider low-energy state configurations of QCA circuits. However, current QCA simulators compute just the ground state configuration of a QCA arrangement. In this paper, we offer an efficient method, based on graphical probabilistic models, to compute the N-lowest energy modes of a clocked QCA circuit. The overall low-energy, excited, spectrum of multiple clocking zones is constructed by concatenating the excited spectra of the individual clocking zones. We demonstrate the use of this error model by comparing different designs of wire crossings.**

## I. Introduction

In quantum-dot cellular automata (QCA) [1] architecture the elementary unit of computation is a cell consisting of two electrons that can exist in four possible quantum dots. There are two possible ground state (minimum energy) configurations for each cell, corresponding to the two possible diagonal occupancies (see Fig. 1). These two states are used to represent the logic states 0 and 1. While there is quantum tunneling between dots in the same cell, there is no quantum tunneling between neighboring cells. However, neighboring cells effect each other by modifying the potential energies through Coulombic interactions, which in turn effect the ground state configuration of a cell arrangement. The kink energy between two cells is defined to be the difference in energy if the cells have opposite states (or polarizations) and the energy if the cells have same states (or polarizations). Thus, a linear arrangement of cells has two ground state configurations, without any kinks, and can act as a wire (see Fig. 1). Another basic logic element is the 3-input majority gate that can be constructed by arranging the cells as shown in Fig. 1. Logic circuits can be built by mapping the intended logic onto the ground state configuration.

Initial criticisms about the difficulty of converging to the ground state has been solved by using the concept of a four phased adiabatic clocking. In such designs, the overall circuit is divided into zones, with each zone driven by one of the four clocks. The clocks are phase shifted versions of each other. The clocking scheme controls the flow of information in a QCA circuit by driving each cell through depolarized state, latching phase, and hold phase, and then back to a depolarized

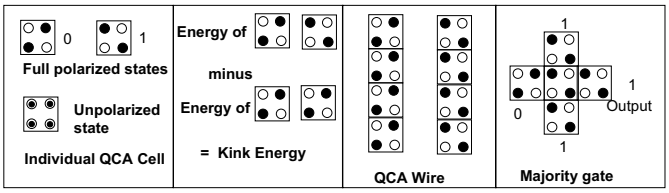


Fig. 1. QCA basics and the traditional use of QCAs for logic computing. Each cell exists in a combination of two polarized states. The kink energy between two cells is defined to be the difference in energy if the cells have opposite states and the energy if the cells have same states. A linear arrangement of cells has two ground state configurations and can act as a wire. Majority logic is natural to QCA and is the basic gate for QCA circuits.

state. A depolarized cell state does not effect the surrounding cells. The clock phases of two consecutive zones are staggered so that the cells in one zone can "drive" the cells in the other zone. The adiabatic aspect of the clocking seeks to keep the circuit at ground state. Since there is no flow of electrons involved, there is no need for interconnects, and it has potential for extremely low-power computing.

Apart from fabrication related defects and hard faults [2], there are four kinds of soft errors in QCA operations: decay errors, dynamic errors, background charge fluctuations, and switching (or thermal) errors. There were analyzed and experimentally quantified for metal-dot QCAs in [3] and expected to be also present for molecular QCAs. Decay error occurs due to the failure of retaining the state of a cell, however, the time constants of such effects is larger than the GHz operating point of QCA clocks. Dynamic errors can occur when the clock frequencies approach the time constants for tunneling events. Thus, this would be a problem only for ultra high frequencies ($>>$ 1 GHz). Random background charge drifts in the order of minutes could be a problems, but there is possibility that new fabrication methods can control it. By far, the most dominant form of errors in QCA devices are expected to be switching or thermal errors. Within each clocking zone it is necessary that the cells stay in the ground state. This can be achieved by using adiabatic clocking so that states are not changed suddenly. However in practice, imperfect adiabatic clocking and increased temperatures can results in error conditions when the cells in a zone can settle down to a excited states. At temperature $T$, the probability for these kinds of thermally induced errors is given by [3]: $p_{th} \propto \exp(-\Delta/kT)$, where $k$ is the Boltzman constant and $\Delta$ is the energy gap between the ground state and the next excited state. Thus, to analyze these switching errors in QCA circuits, we need to be able

1-4244-0078-3/06/$20.00 (c) 2006 IEEE

to reason about near ground states in each clocking zone. However, current QCA simulators (the best available is [4]) cannot compute such states. The only work that computes the non-ground state is [5], but it computes just one lowest energy state configuration that causes output errors. It cannot find all the degenerate states, i.e. multiple states with same energy, and it does not provide a clock zone by clock zone energy spectrum. *To fully study the error behavior of designs it is important to consider excited states in each clocking zone.*

The inference of the low-energy non-ground states requires an exploration of the QCA cell state configuration space, whose size is exponential in the number of cells in each clocking zone. The only currently available approach, that we are aware, to accomplish this is using simulated annealing search [6], which is time consuming. For a circuit with 6 cells, it can take 10,000's of iteration. In this paper, we present a method based on maximum likelihood probabilistic inference to infer the $N$-lowest energy configurations. The inference is conducted with a graphical probabilistic model [7] that is built to represent the joint probability of the state configuration. The $N$-most likely states correspond to the $N$-lowest energy states.

## II. Markov Model of QCA Computation

We denote a QCA cell is denoted by $X_i$, where $i = 1, \cdots, N$. The first $r$ cells, $\{X_1, \cdots, X_r\}$ are the driving cells, and the next $N-r$ cells, $\{X_{r+1}, \cdots, X_N\}$ are the driven cells. The driver cells are the cells in the previous clock zone or are the primary inputs for the first clock zone. Each cell can be observed to be in a one of a finite number of states, $x_i$. If we consider just the ground states of the cell, then there will be 2 of them, denoting a 0 or a 1. We will denote the probability of *observing* a cell at state, $x_i$, by $P(X_i = x_i)$ or $P_{X_i}(x_i)$, or simply by $P(x_i)$. The commonly used attribute of a *polarization* of a QCA cell can be expressed in terms of these state probabilities, $\rho_{X_i} = P_{X_i}(1) - P_{X_i}(0)$. The joint probability of observing a set assignments for the cells is denoted by $P(x_1, \cdots, x_n)$. The probability of state assignment of a $N$-cell arrangement is determined by the Boltzman distribution law. Thus,

$$P(x_1, \cdots, x_N) = \frac{1}{Z} \exp\left(-\frac{E(x_1, \cdots, x_N)}{kT}\right) \quad (1)$$

where $Z$ is the normalizing partition function, $k$ is the Boltzman constant, and $T$ is the temperature. The function $E(x_1, \cdots, x_N)$ is the energy of the state assignment. If we consider only Coulombic interactions between QCA-cells, ignoring quantum effects within cells, this energy would be composed out of energy terms capturing energy between two QCA cells, $E(x_i, x_j)$. It is not necessary to model the interactions of each cell with every other cells. Due to the $1/r^5$ fall-off of Coulombic interaction between cells, the energy term between the pair of cells that are far away can be ignored. Let $Ne(X)$ represent the set of cells that are within a specified distance, $D$, from it, then the total energy can be expressed as

$$E(x_1, \cdots, x_n) = \sum_{i=1}^{N} \sum_{j=Ne(X_i)} E(x_i, x_j) \quad (2)$$

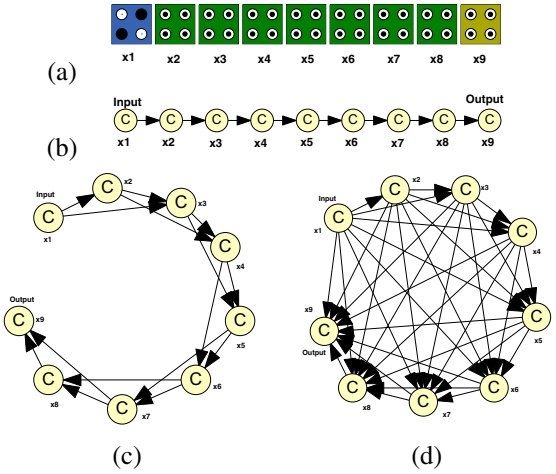


Fig. 2. Markov net dependency model for (a) 9-cell QCA wire considering (b) 1-cell radius of influence (b) 2-cell radius of influence, and (c) all cells. *Ignore the link directions.*

where $Ne(X_i) = \{X_j | d(X_i, X_j) \leq D\}$ and $d$ is the Euclidean distance function. This decomposition of the total energy in a set of pairwise interactions, induces a decomposition of the joint probability function.

$$P(x_1, \cdots, x_M) = \frac{1}{Z} \exp\left(-\frac{\sum_{i=1}^{M} \sum_{j=Ne(X_i)} E(x_i, x_j)}{kT}\right) \quad (3)$$

This joint probability can be factored in terms of pairwise functions, which we will term as probability potential functions, $\phi(x_i, x_j) = \exp\left(-\frac{E(x_i, x_j)}{kT}\right)$.

$$P(x_1, \cdots, x_M) = \frac{1}{Z} \prod_{i=1, j=Ne(X_i)}^{i=M} \phi(x_i, x_j) \quad (4)$$

Given this joint probability function, in principle, it is possible to compute probability of any state configuration or the marginal probability of any particular subset of random variables. However, the computational complexity is exponential if the computations are blind to independencies that exist because of the local nature of the Coulombic interactions. We exploit these independencies to *factorize* the underlying joint probability function into product of joint probability functions over smaller subsets of random variables. We do not have space to describe this factorization process in detail. However it suffices to say that it involves the construction of a Markov graph network, followed by a process called graph triangulation, followed by the construction of a tree of cliques. More details of the later two processes can be found in [7]. Fig. 2 shows an illustration of the mapping of a QCA cell arrangement to a Markov network. The Markov graph representation for 1-cell and 2-cell radius of influence are shown in Figs. 2(b) and (c), respectively. Fig. 2(d) shows a 9-cell neighborhood, where there is no approximation about the neighborhood of influence – we have a complete graph.

Markov models are commonly used in reliability studies of circuits [8], [9], where average case behavior is computed. We

take this idea farther by (i) exploring non-ground states using maximum-likelihood inference rather than average-likelihood, (ii) strongly coupling device physics into the model, (iii) and using an accurate probabilistic computing model.

## III. Error Modes of Each Clock Zone

Given the joint probability specification of the cells in these two zones $P(X_1 = x_1, \cdots, X_n = x_n)$, as captured by the Markov network representation, we explore the computation of the following:

1) Given the polarization of the driver cells in the previous clock zone, $x_1, \cdots, x_r$, what is the *minimum energy* polarization (or most likely state) assignments of all the cells? For this we need to compute $\arg\max_{x_1, x_2, \cdots} P(x_{r+1}, \cdots, x_N | x_1, \cdots, x_r)$, or the maximum likelihood state assignments.
2) What are N-lowest energy configuration for the QCA circuit, for a given driver cell configuration, $x_1, \cdots, x_r$?

Note that these computations are different from the computation of the average case (expected) probabilities, or marginal probabilities, which is commonly considered in most probabilistic analysis. We need *maximum likelihood inference*. The answer to the first question above can be arrived by message passing in the graphical dependency structure that we construct among the QCA cells. We refer the reader to [7] for details about the details of the inference scheme that is involved. The inference scheme is an exact one and is guaranteed to result in the global maximum. However, to also arrive at the N-most probable configurations (question 2 above), we adopt the iterative strategy proposed by [10], [7], starting from the most probable configuration found by maximum likelihood inference.

The search for the $k$-th lowest energy configuration is constrained by the 1-st through $k-1$-th lowest energy configurations found. Let the most likely configuration of variables be denoted by $\mathbf{x}^{(1)} = \{x_1^1, \cdots, x_N^1\}$, with a probability of $P^*(\mathbf{x}^{(1)})$. The second most likely configuration, $\mathbf{x}^{(2)}$ must differ from the most likely configuration in the state of at least one variable. We search for this configuration by performing $N$ maximum propagations with the evidences, $F_i$, given by

$$F_i = \{X_1 = x_1^1, \cdots, X_{i-1} = x_{i-1}^1, X_i \neq x_i^1\} \tag{5}$$

for $i = 1, \cdots, N$. Let the mostly likely configuration, constrained by the evidence, $F_i$, be $\mathbf{x}^{(F_i)}$ with probability $P^*(\mathbf{x}^{(F_i)})$. The second most likely configuration will be the most likely configuration with one of these evidences.

$$\mathbf{x}^{(2)} = \arg\max_{\mathbf{x}^{(F_i)}} P^*(\mathbf{x}^{(F_i)}) \tag{6}$$

The third most likely configuration, $\mathbf{x}^{(3)}$, will be from this set of propagations, i.e. one of $\mathbf{x}^{(F_j)}$, or from propagations with evidences that differ from the first and second most likely configurations by at least one state each, $F_{ij}$.

$$F_{ij} = \{X_1 = x_1^1, \cdots, X_{i-1} = x_{i-1}^1, X_i \neq x_i^1, X_{i+1} = x_{i+1}^1, \cdots, X_j \neq x_j^2\} \tag{7}$$

for $j = 1, \cdots, N-i+1$. Thus, the third most likely configuration is

$$\mathbf{x}^{(3)} = \arg\max \left( \max_{\mathbf{x}^{(F_i)}} P^*(\mathbf{x}^{(F_i)}), \max_{\mathbf{x}^{(F_{ij})}} P^*(\mathbf{x}^{(F_{ij})}) \right) \tag{8}$$

The process continues, until we have $N$ most likely configurations.

## IV. Energy Spectrum of Multiple Clocked Zones

To construct the energy spectrum of the full clocked QCA circuit, we use the Markov model based inference mechanism for each clock zone, *conditioned* on the low-energy states of the previous clock zone. For the first clock zone, we compute the ground and excited states. For the second clock zone, we compute the ground and excited states conditioned once on the first zone in the ground state and then conditioned on the first zone in the excited state. Thus, for the second zone, we have four possible sets of states. The possible ground and exited states for a clock zone increases with this distance from the primary inputs. This defines a state configuration tree for clocked QCA circuits.

## V. Results

We illustrate our ideas using QCA crossbars, a crucial element of QCA circuits. The ability to cross wires in QCA designs has been considered to be one its biggest advantages. Consider the arrangement of QCA cells shown in Fig. 3(a), which shows three vertical QCA wires consisting of rotated cells and one horizontal wire. Since the horizontal wire is "cut" by the vertical wire, errors in the horizontal wire is of concern. Figs. 3(b), (c), and (d) shows three switching error modes. Fig. 3(e) shows the excited spectrum of the design. It plots the probability of each of the excited state configurations. The configurations that result in output errors are marked by red bars. Note that ground state (the left most bar) is not the only one resulting in correct output; switching errors can "cancel out" to result in correct output, however, the associated probabilities would be low. Notice that first excited states of the design is almost as probable as the ground state. Also, there are three excited states. All of this suggests that the design is unstable and prone to switching errors. This corroborates the finding of crossbar instability in [11].

To harden the design, we use the pattern of the switching error modes in Figs. 3(b), (c), and (d) to partition the circuit into 4 clock zones as shown in Fig. 4(a). In addition we considered hardening the design at the crossings by thickening them (Fig. 4(b)) and also adding clocking zones (Fig. 4(c)). To characterize the overall switching stability of a circuit, we will use the ratio of the probability of the error state configurations to the configurations that results in correct output.

$$L^{(i)} = \frac{\sum_{(i) \in \text{error}} \Pr(x^{(i)})}{\sum_{(j) \in \text{correct}} \Pr(x^{(j)})} \tag{9}$$

*We call this ratio the switching error likelihood $L^{(i)}$ and suggest it as design metric. The lower this value, the better.* Higher values indicates the propensity of switching errors.

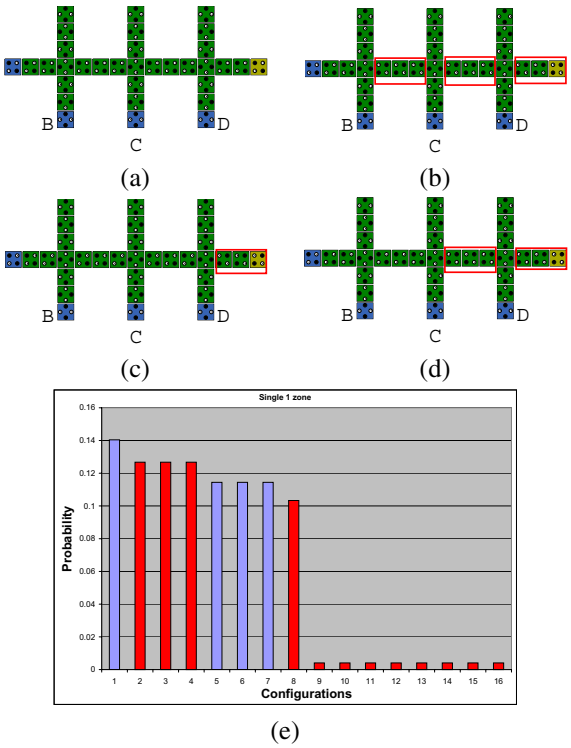


Fig. 3. (a) Consecutive crossbars, all in one clock zone. Errors in the horizontal line are of concern. The switching error modes are shown in (b), (c), and (d). The excited state spectrum for the design is shown in (e). The bars corresponds to the probability of that configuration. The configurations that result in output errors are denoted by red bars.

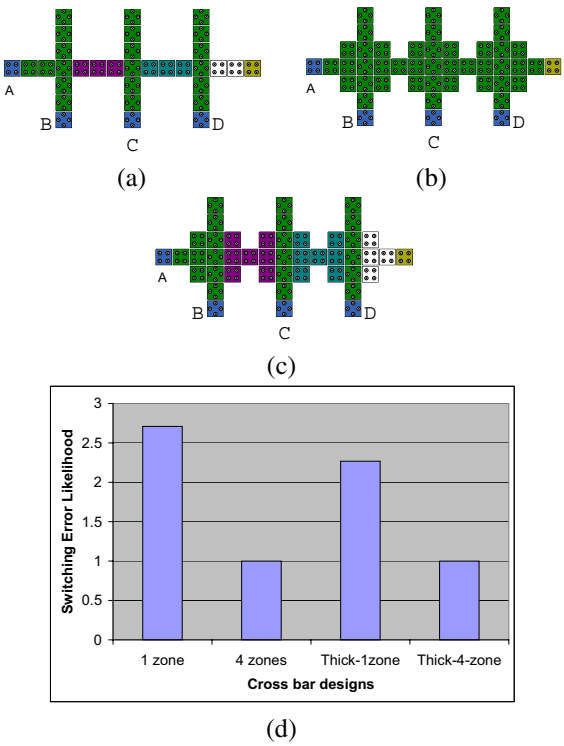


Fig. 4. Different crossbar designs with three crossings (a) clocked single cell in 4 clock zone, (b) thickened crossings – all in one clock zone, (c) thickened crossings with 4 clock zones. (d) Switching error likelihood of different crossbar designs.

Fig. 4(d) plots the value of this ratio for the four crossbar designs. We notice that with thickened crossing, the switching error propensity goes down even with one clocking zone. However, the greatest gain is the addition of clocking zone. The switching error likelihood for thickened and single cell design is similar with addition of clocking zones. We also noticed that the switching error modes of all the four designs are the same, except for the error likelihood values.

## VI. Conclusions

We described an efficient computation mechanism to estimate switching error likelihoods in clocked QCA circuits. To our knowledge, this is the first such formalism proposed at circuit level. The analysis is based on inferring the excited states of each clocking zone and constructing a configuration tree for the whole circuit. We modeled any QCA cell arrangement using a Markov graph-based probabilistic model, which we then transformed into a Markov tree structure defined over subsets of QCA cells. The N-lowest energy configurations were then computed by local message passing; the inference is exact and there are no approximations involved. We demonstrated the model using crossover wire designs. The developed method should be useful in the analysis and design of robust QCA circuits in terms of switching errors in the presence of variabilities in permitivity, cell size, defects, and operating temperature.

## References

[1] C. S. Lent, P. D. Tougaw, and W. Porod, "Quantum cellular automata: the physics of computing with arrays of quantum dot molecules," in *The Proceedings of the Workshop Physics and Computing*, pp. 5–13, 1994.

[2] M. Momenzadeh, J. Huang, M. Tahoori, and F. Lombardi, "On the evaluation of scaling of QCA devices in the presence of defects at manufacturing," *IEEE Trans. on Nanotechnology*, vol. 4, pp. 740–743, Nov. 2005.

[3] R. Kummamuru, A. Orlov, R. Ramasubramaniam, C. Lent, G. Bernstein, and G. Snider, "Operation of a quantum-dot cellular automata (qca) shift register and analysis of errors," *IEEE Transactions on Apllied Physics*, vol. 50, pp. 1906–1913, September 2003.

[4] K. Walus, T. Dysart, G. Jullien, and R. Budiman, "QCADesigner: A rapid design and simulation tool for quantum-dot cellular automata," *IEEE Trans. on Nanotechnology*, vol. 3, pp. 26–29, March 2004.

[5] S. Bhanja and S. Sarkar, "Graphical probabilistic inference for ground state and near-ground state computing in QCA circuits," in *IEEE Conference on Nanotechnology*, 2005.

[6] M. Macucci, G. Iannaccone, S. Francaviglia, and B. Pellegrini, "Semiclassical simulation of quantum cellular automaton circuits," *Intl. Journal of Circuit Theory and Application*, vol. 29, pp. 37–47, 2001.

[7] R. G. Cowell, A. P. David, S. L. Lauritzen, and D. J. Spiegelhalter, *Probabilistic Networks and Expert Systems*. New York: Springer-Verlag, 1999.

[8] Y. Qi, J. Gao, and J. Fortes, "Markov chains and probabilistic computation: A general framework for multiplexed nanoelectronic systems," *IEEE Trans. Nanotechnology*, vol. 4, pp. 194–205, Mar. 2005.

[9] K. Nepal, I. Bahar, J. Mundy, W. R. Patterson, and A. Zaslavsky, "Designing mrf based error correcting circuits for memory elements," in *Design, Automation and Test Conference*, 2006.

[10] D. Nilsson, "An efficient algorithm for finding the m most probable configurationsin probabilistic expert systems," *Statistics and Computing*, vol. 8, pp. 159–173, June 1998.

[11] K. Walus and G. A. Jullien, "QCA co-planar wire-crossing and multilayer networks," in *iCore Banff Summit*, (Banff, Alberta), June 2004.